Research Square

Preprints are preliminary reports that have not undergone peer review.
They should not be considered conclusive, used to inform clinical practice,
or referenced by the media as validated information.

The gut microbiota-derived tryptophan metabolite indole-3-propionic acid attenuates bupivacaine-induced neuronal injury in rats

Faruk Furkan Bank

farukfurkan.bank@deu.edu.tr

Dokuz Eylül University

Hale Aksu

Dokuz Eylül University

Serap Cilaker Micili

Dokuz Eylül University

Selin Nur Cetin

Dokuz Eylül University

Beste Balbal

Dokuz Eylül University

Sefa Kizildag

Dokuz Eylül University

Volkan Hanci

Dokuz Eylül University

Research Article

Keywords: Indole-3-propionic acid, Tryptophan metabolism, Gut–brain axis, Bupivacaine, Neuroprotection, Apoptosis

Posted Date: November 24th, 2026

DOI: https://doi.org/10.21203/rs.3.rs-11839670/v1

License: This work is licensed under a Creative Commons Attribution 4.0 International License.
Read Full License

Additional Declarations: No competing interests reported.

The gut microbiota-derived tryptophan metabolite indole-3-propionic acid attenuates bupivacaine-induced neuronal injury in rats

Faruk Furkan Bank[1], Hale Aksu[1], Serap Cilaker Micili[2], Selin Nur Cetin[2], Beste Balbal[3], Sefa Kizildag[3], Volkan Hanci[1]

[1]Department of Anesthesiology and Reanimation, Faculty of Medicine, Dokuz Eylul University, Izmir, Türkiye

[2]Department of Histology and Embryology, Faculty of Medicine, Dokuz Eylul University, Izmir, Türkiye

[3]Department of Medical Biology and Genetics, Institute of Health Sciences, Dokuz Eylul University, Izmir, Türkiye

Corresponding author: Faruk Furkan Bank, MD, Department of Anesthesiology and Reanimation, Faculty of Medicine, Dokuz Eylul University, Balcova, 35340 Izmir, Türkiye. E-mail: farukfurkan.bank@deu.edu.tr

ORCID iDs

Faruk Furkan Bank: 0000-0002-8658-3475

Hale Aksu: 0000-0002-4887-1337

Serap Cilaker Micili: 0000-0002-9830-0989

Selin Nur Cetin: 0009-0002-3896-1256

Beste Balbal: 0000-0003-1407-2497

Sefa Kizildag: 0000-0001-7939-5153

Volkan Hanci: 0000-0002-2227-194X

Acknowledgements: None.

Abstract

Local anesthetic systemic toxicity is a life-threatening complication of regional anesthesia in which bupivacaine injures neurons through direct neurotoxic and secondary ischemic mechanisms, and lipid emulsion offers limited neuronal cytoprotection. Indole-3-propionic acid, a gut microbiota-derived tryptophan metabolite with antioxidant, anti-apoptotic and anti-inflammatory activity, is neuroprotective in ischemic and neurodegenerative models but has not been examined in local anesthetic toxicity. Thirty-two female Wistar albino rats were studied; 30 completed the protocol and were allocated to five groups (n=6 each): control, bupivacaine, bupivacaine with lipid emulsion, bupivacaine with indole-3-propionic acid (10 mg/kg intraperitoneally), and combined treatment. Bupivacaine 0.5% was infused intravenously at 1 mg/kg/min until death. Survival time, neuronal density in the prefrontal cortex and hippocampus, and markers of apoptosis (Bcl-2, Bax, caspase-3, cytochrome c) and inflammation (tumor necrosis factor-α) were assessed at the transcript and protein levels. Survival differed across groups (P=0.029); only combined treatment prolonged survival versus untreated bupivacaine (15.33±4.55 vs. 9.83±1.72 min, P=0.017). Prefrontal cortex neuronal density was higher with indole-3-propionic acid than with untreated bupivacaine (40.12±0.47% vs. 29.31±0.59%, P<0.001), and combined treatment approached control values (46.63±0.58%, P<0.0001 versus bupivacaine). Indole-3-propionic acid raised the Bcl-2/Bax mRNA ratio to 9.25-fold of control and reduced tumor necrosis factor-α mRNA to 0.70-fold (both P<0.0001 versus bupivacaine), and both changes were confirmed at the protein level. In this model, indole-3-propionic acid attenuated bupivacaine-induced neuronal injury through anti-apoptotic and anti-inflammatory mechanisms. These findings are hypothesis-generating and require further investigation before clinical inference.

Keywords Indole-3-propionic acid · Tryptophan metabolism · Gut–brain axis · Bupivacaine · Neuroprotection · Apoptosis

Introduction

Local anesthetic systemic toxicity (LAST) represents a potentially life-threatening complication of regional anesthesia, with an estimated incidence of 0.03–0.1% in peripheral nerve blocks (Gitman and Barrington 2018; Vasques et al. 2015; El-Boghdadly and Chin 2016). Bupivacaine (BPV), an amide-type local anesthetic widely used for its prolonged duration of action, carries the highest cardiotoxicity risk among commonly employed agents (Bern and Weinberg 2011). Central nervous system toxicity, which arises largely from rising plasma concentrations, often precedes cardiovascular collapse; in its most severe form BPV toxicity culminates in cardiac arrest, after which global cerebral hypoperfusion compounds any direct neuronal injury and may result in permanent neurological sequelae (Verlinde et al. 2016). The resulting encephalopathy is therefore of mixed toxic and metabolic origin, combining drug-induced mitochondrial impairment with the energy failure that follows circulatory arrest.

At the cellular level, BPV can exert direct neurotoxicity that is distinct from plasma concentration-dependent central nervous system excitation; proposed mechanisms include mitochondrial dysfunction, oxidative stress, and activation of apoptotic cascades (Yang et al. 2011; Perez-Castro et al. 2009; Werdehausen et al. 2007). Key molecular pathways implicated include the B-cell lymphoma 2 (Bcl-2) family proteins, which regulate intrinsic apoptosis through the balance between pro-survival Bcl-2 and pro-apoptotic B-cell lymphoma 2-associated X protein (Bax) (Youle and Strasser 2008). Downstream effectors such as caspase-3 and cytochrome c execute the final stages of programmed cell death (Li and Yuan 2008).

Current treatment of LAST relies primarily on supportive care and intravenous lipid emulsion (LE) therapy. Although historically attributed to a ‘lipid sink’ that sequesters lipophilic local anesthetics, the benefit of LE is now understood to involve multiple mechanisms, including a volume effect and direct cardiotonic actions, in addition to partitioning (Weinberg et al. 1998; Rosenblatt et al. 2006; Neal et al. 2018). Nevertheless, LE provides limited direct cytoprotection at the neuronal level, and novel adjunctive therapies targeting the underlying cellular damage mechanisms are needed (Ok et al. 2018).

Microbial metabolism of dietary tryptophan generates a family of circulating indole derivatives that reach the brain and modulate neuronal survival, placing the gut–brain axis among the metabolic determinants of brain injury (Wikoff et al. 2009; Dodd et al. 2017; Roager and Licht 2018). Indole-3-propionic acid (IPA), produced primarily by *Clostridium sporogenes*, has emerged from this group as a potent endogenous neuroprotectant and demonstrates superior hydroxyl radical scavenging capacity compared with melatonin and other established antioxidants (Chyan et al. 1999). Its neuroprotective effects have been documented in models of ischemia-reperfusion injury, Alzheimer’s disease, and oxidative stress-induced neuronal damage (Hwang et al. 2009; Bendheim et al. 2002), mechanisms relevant to both the oxidative and ischemic components of local anesthetic-induced neuronal injury. Circulating IPA concentrations also track systemic metabolic state and cognitive outcome in experimental models (Liu et al. 2020). However, its activity in the setting of local anesthetic toxicity has not previously been examined; to our knowledge, no prior study has investigated a gut microbiota-derived tryptophan metabolite in the context of LAST.

This study aimed to investigate whether IPA confers neuroprotection against BPV-induced neuronal injury in rats, examining both histopathological outcomes and molecular markers of apoptosis and inflammation. We hypothesized that IPA, either alone or in combination with LE, would attenuate BPV-associated neuronal injury through anti-apoptotic and anti-inflammatory mechanisms.

Materials and methods

Ethical approval and study design

This prospective, randomized, controlled experimental study was approved by the Dokuz Eylul University Animal Experiments Local Ethics Committee, Izmir, Türkiye (protocol no. 01/2025; approval date: 22 January 2025). All procedures were carried out in accordance with the WHO International Guiding Principles for Biomedical Research Involving Animals, the Guide for the Care and Use of Laboratory Animals (National Institutes of Health), the national legal requirements and guidelines for the care and use of laboratory animals in force in Türkiye, the European Directive 2010/63/EU, and the ARRIVE 2.0 reporting guidelines; the completed ARRIVE checklist is provided as supplementary material. Animal preparation and induction of bupivacaine toxicity were performed at

the Dokuz Eylul University Laboratory Animal Science Department; histopathological analyses, molecular analyses (real-time quantitative polymerase chain reaction and Western blot), and statistical analysis were completed subsequently.

Animals and housing

Thirty-two female Wistar albino rats (246–288 g, 10–12 weeks old) were obtained from the Dokuz Eylul University Laboratory Animal Science Department, Izmir, Türkiye. Animals were housed in standard polycarbonate cages (four per cage) under controlled conditions (22±2 °C, 50–60% humidity, 12:12 h light–dark cycle) with ad libitum access to standard rodent chow and water. Only female animals were studied; the potential influence of sex on the outcomes was therefore not assessed and is addressed as a limitation.

Randomization and blinding

Healthy female Wistar albino rats within the specified weight range were eligible for inclusion; animals that died from anesthesia-related causes before completion of the toxicity protocol were excluded. These criteria were defined a priori. Two of the 32 animals died from high-dose anesthesia before completion of the toxicity protocol and were excluded on this basis, leaving 30 animals (six per group) for analysis; no further data were excluded. Animals were randomly allocated to five experimental groups (n=6 for each group) using a random number table: Group 1 (Control), 1 mL/kg 0.9% saline intraperitoneally; Group 2 (BPV), BPV toxicity without treatment; Group 3 (BPV+LE), BPV toxicity with 20% LE treatment (3 mL/kg/min for 5 minutes); Group 4 (BPV+IPA), BPV toxicity with IPA treatment (10 mg/kg intraperitoneally); Group 5 (Combined), BPV toxicity with sequential LE and IPA treatment. Histopathological sections were examined by two investigators from the Department of Histology and Embryology who were blinded to group allocation.

Experimental protocol

Anesthesia was induced using 5% sevoflurane in 3 L/min oxygen via induction chamber. Adequate anesthesia depth was confirmed by absent tail-pinch response. Tail vein catheterization was performed for intravenous drug administration, tail artery cannulation for hemodynamic monitoring, and electrocardiographic monitoring was established using subcutaneous needle electrodes. In the control group, animals received 1 mL/kg 0.9% saline intraperitoneally and were observed for 30 minutes before euthanasia under high-dose sevoflurane anesthesia. In toxicity groups (Groups 2–5), 0.5% isobaric BPV was infused intravenously at 1 mg/kg/min. Importantly, BPV infusion was continued without interruption throughout the experiment until death (cardiac arrest) occurred, representing a lethal toxicity model. Convulsive activity and cardiac rhythm were continuously monitored and recorded. Upon first observation of convulsive activity, treatment interventions were administered while BPV infusion continued: Group 3 received 20% LE at 3 mL/kg/min for 5 minutes intravenously; Group 4 received IPA 10 mg/kg intraperitoneally; Group 5 received LE followed by IPA sequentially. IPA solution was freshly prepared by dissolving powdered indole-3-propionic acid (Sigma-Aldrich, St. Louis, MO, USA) to achieve a concentration of 10 mg/mL using a precision balance, and was administered intraperitoneally at a volume of 1 mL/kg to deliver the target dose of 10 mg/kg. The IPA dose (10 mg/kg, intraperitoneal) was selected based on previously reported effective intraperitoneal dosing of indole-3-propionic acid in rodent neuroprotection models (Liu et al. 2020). Survival time, defined as the interval from BPV infusion initiation to death, was recorded for all toxicity groups. All observed neurological and cardiological findings were documented on standardized data collection forms.

Tissue collection and processing

Following death in toxicity groups or euthanasia in controls, brains were rapidly excised and rinsed with ice-cold saline solution. The brain was hemisected; the right hemisphere was fixed in 10% neutral buffered formalin for histopathological analysis. From the left hemisphere, prefrontal cortex and hippocampal regions were dissected, placed in RNAlater-ICE Frozen Tissue Transition Solution (500 mg tissue per 2.5 mL solution; Invitrogen, Thermo Fisher Scientific, Waltham, MA, USA; cat. no. AM7030), and stored at −80 °C for subsequent molecular analyses.

Histopathological analysis

Fixed tissues were paraffin-embedded, sectioned at 5 μm thickness, and stained with hematoxylin and eosin. Sections were examined independently by two investigators from the Department of Histology and Embryology

who were blinded to group allocation and who had no involvement in the animal experiments. Neuronal damage was assessed semi-quantitatively in the prefrontal cortex and hippocampal CA1–3 region, evaluating cellular morphology, nuclear condensation, cytoplasmic eosinophilia, and tissue architecture.

Real-time quantitative polymerase chain reaction

Total ribonucleic acid (RNA) was extracted using PureZOL RNA Isolation Reagent (Bio-Rad Laboratories, Hercules, CA, USA; cat. no. 7326890) according to the manufacturer's protocol. RNA quality and concentration were assessed spectrophotometrically (A260/A280 ratio >1.8). Complementary deoxyribonucleic acid was synthesized from 1 μg total RNA using iScript Reverse Transcription Supermix for RT-qPCR (Bio-Rad Laboratories, Hercules, CA, USA; cat. no. 1708840) according to the manufacturer's instructions. Real-time quantitative polymerase chain reaction (RT-qPCR) was performed using SsoAdvanced Universal SYBR Green Supermix (Bio-Rad Laboratories, Hercules, CA, USA). Target genes included Bcl-2, Bax, caspase-3, cytochrome c, and tumor necrosis factor-α (TNF-α). Glyceraldehyde 3-phosphate dehydrogenase (GAPDH) served as the reference gene. Relative expression was calculated using the $2^{-\Delta\Delta Ct}$ method (Livak and Schmittgen 2001).

Western blot analysis

Protein was extracted using radioimmunoprecipitation assay buffer containing protease inhibitors. Protein concentrations were determined using a bicinchoninic acid protein assay kit (Takara Bio, Kusatsu, Shiga, Japan; cat. no. T9300A). Equal amounts (30 μg) were separated on 10% TGX Stain-Free FastCast gels (Bio-Rad Laboratories, Hercules, CA, USA; cat. no. 1610183) by sodium dodecyl sulfate-polyacrylamide gel electrophoresis and transferred to polyvinylidene difluoride (PVDF) membranes using a Trans-Blot Turbo Mini PVDF transfer pack (Bio-Rad; cat. no. 1620177). Membranes were blocked with fish gelatin blocking buffer (Takara Bio; cat. no. T7131A) and probed with rabbit polyclonal primary antibodies against Bcl-2 (Proteintech, Rosemont, IL, USA; cat. no. 26593-1-AP) and TNF-α (Proteintech; cat. no. 17590-1-AP), together with commercially available primary antibodies against Bax and β-actin (loading control). Horseradish peroxidase-conjugated AffiniPure goat anti-rabbit IgG (H+L) (Proteintech; cat. no. SA00001-2) and goat anti-mouse IgG (H+L) (Proteintech; cat. no. SA00001-1) were used as secondary antibodies. Chemiluminescent detection was performed with Clarity Western ECL substrate (Bio-Rad; cat. no. 1705061), and band intensities were quantified using ImageJ software (National Institutes of Health, Bethesda, MD, USA; RRID:SCR_003070).

Statistical analysis

The sample size of six animals per group was based on group sizes commonly used in comparable experimental rat models of local anesthetic toxicity and on the 3Rs principle of reducing animal use, while retaining sufficient sensitivity to detect large between-group differences in the primary histopathological outcome. Data are expressed as mean±standard deviation, except neuronal density and molecular marker data (Table 1, Figs. 4 and 5), which are presented as mean±standard error of the mean. Normality was assessed using the Shapiro–Wilk test and homogeneity of variance using Levene's test. Normally distributed data were analyzed using one-way analysis of variance (ANOVA) with Tukey's post-hoc test for multiple comparisons; non-normally distributed data were analyzed using the Kruskal–Wallis test with Dunn's correction. Survival time was treated as a continuous variable and compared using one-way ANOVA with Tukey's post-hoc test. Statistical significance was set at $P<0.05$, and significance levels are indicated in Figs. 1–5 as $P<0.05$, $P<0.01$, $P<0.001$ and $P<0.0001$. All statistical analyses were performed and all graphs were created using GraphPad Prism version 9.0 (GraphPad Software, San Diego, CA, USA); photomicrographs were assembled and neuronal density was quantified using ImageJ software (National Institutes of Health, Bethesda, MD, USA; RRID:SCR_003070).

Results

Baseline characteristics and homogeneity

Of 32 rats initially included, two died due to high-dose anesthesia, leaving 30 rats (six per group) for analysis. Baseline body weights did not differ significantly between groups ($P=0.060$), confirming successful randomization. Body weights ranged from 254.17±3.76 g in the Control group to 271.0±12.3 g in the BPV plus LE group.

Survival analysis

Survival time differed significantly across groups (one-way ANOVA, P=0.029). The BPV group had the shortest survival time (9.83±1.72 minutes). Combined LE and IPA treatment was the only group with a significantly longer survival time than BPV alone (15.33±4.55 minutes, P=0.017, Tukey's post-hoc test). IPA monotherapy (12.83±2.04 minutes, P=0.300) and LE monotherapy (12.17±2.32 minutes, P=0.512) each produced numerically longer survival times that did not reach statistical significance versus BPV.

Histopathological findings

Neuronal density analysis revealed region-specific patterns of injury and protection (Table 1). In the prefrontal cortex, BPV reduced neuronal density relative to control (29.31±0.59% vs. 46.01±0.47%, P<0.05). All three treatment groups showed greater neuronal density than untreated BPV, and the magnitude of this difference increased across treatments: LE (39.21±0.95%, P<0.01), IPA (40.12±0.47%, P<0.001) and combined treatment (46.63±0.58%, P<0.0001). Values in the combined treatment group did not differ from control (Fig. 1).

In the hippocampal CA1 region, BPV reduced neuronal density compared with control (44.02±2.26% vs. 54.02±2.04%, P<0.05). Only combined treatment differed significantly from untreated BPV (50.31±1.21%, P<0.01); neither LE (50.00±4.81%) nor IPA (49.81±1.08%) alone reached significance, although both showed numerically higher values than BPV (Fig. 2). In the hippocampal CA3 region, BPV again reduced neuronal density relative to control (38.60±2.52% vs. 46.70±0.30%, P<0.05), but none of the treatment groups differed significantly from untreated BPV, suggesting regional variation in treatment responsiveness (Fig. 3).

Molecular analyses

To elucidate the molecular mechanisms underlying the observed neuroprotection, apoptotic and inflammatory markers were analyzed at both transcriptional and translational levels.

Gene expression analysis

RT-qPCR analysis revealed that IPA treatment profoundly modulated apoptotic gene expression. The anti-apoptotic Bcl-2/Bax mRNA ratio reached 9.25-fold of control in the BPV+IPA group, significantly higher than untreated BPV (P<0.0001) (Fig. 4a). Expression of the pro-apoptotic effector caspase-3 mRNA was substantially suppressed to 0.18-fold of control following IPA treatment (P<0.0001 versus BPV) (Fig. 4b). Cytochrome c mRNA was reduced to 0.46-fold of control (P<0.0001 versus BPV) (Fig. 4c), suggesting preserved mitochondrial membrane integrity. TNF-α mRNA levels were markedly elevated by BPV (2.25-fold of control) and reduced to 0.70-fold of control by IPA (P<0.0001 versus BPV) (Fig. 4d), indicating anti-inflammatory activity in this model.

Protein expression analysis

Western blot analysis confirmed that transcriptional changes were translated to the protein level. The Bcl-2/Bax protein ratio rose to 1.22-fold of control in the IPA-treated group (P<0.0001 versus BPV) (Fig. 5a, b). TNF-α protein expression was elevated in the BPV group compared with control (P<0.01) and compared with BPV+LE (P<0.01); IPA treatment suppressed TNF-α protein levels relative to BPV (P<0.001), whereas values in the combined treatment group remained close to control but did not differ significantly from BPV (Fig. 5c, d).

Discussion

This study demonstrates that IPA attenuates BPV-induced neuronal injury in rats. The protective effects were evidenced by preserved neuronal architecture, upregulation of anti-apoptotic Bcl-2, downregulation of pro-apoptotic Bax and caspase-3, and near-complete suppression of inflammatory TNF-α. To our knowledge, this is the first study to evaluate IPA, or any gut microbiota-derived tryptophan metabolite, in the context of local anesthetic toxicity, extending the therapeutic scope of this endogenous compound beyond the previously studied ischemic and neurodegenerative models. Because BPV was infused until cardiac arrest, the observed neuronal injury reflects a combination of direct local anesthetic neurotoxicity and global hypoxic-ischemic damage secondary to circulatory

arrest; IPA's established activity against ischemia-reperfusion injury is consonant with a protective effect in this combined-injury setting.

Among the survival outcomes, only the combined LE and IPA group showed a significantly longer survival time than untreated BPV (15.33±4.55 vs. 9.83±1.72 min, P=0.017), whereas IPA and LE monotherapies produced numerical but non-significant increases. Because the combined group did not differ significantly from either monotherapy, an additive or synergistic interaction cannot be inferred from these data; the survival findings should therefore be regarded as supportive rather than definitive, with the principal evidence for neuroprotection provided by the histopathological and molecular analyses. The absence of a survival benefit with LE monotherapy warrants explanation. The 'lipid sink' depends on establishing a favorable partition gradient once delivery of the offending agent has ceased; in the present lethal model, BPV was infused continuously until death, so ongoing drug delivery continuously saturated the lipid compartment and prevented an effective gradient. These findings therefore do not contradict the well-established clinical efficacy of LE in LAST but reflect its limitation under sustained, uninterrupted local anesthetic exposure, a deliberately severe model chosen to probe direct cytoprotective effects (Fettiplace and Weinberg 2018; Ozcan and Weinberg 2014; Shi et al. 2013).

IPA's neuroprotective mechanisms appear to be multifaceted. As a potent hydroxyl radical scavenger, IPA neutralizes reactive oxygen species generated during BPV-induced mitochondrial dysfunction and cardiac arrest-related ischemia (Chyan et al. 1999; Hwang et al. 2009; Bendheim et al. 2002). Additionally, our data demonstrate that IPA modulates the Bcl-2/Bax rheostat toward an anti-apoptotic phenotype, consistent with previous reports of IPA's ability to activate pro-survival signaling pathways, including phosphatidylinositol 3-kinase/Akt (Negatu et al. 2020; Zhang et al. 2022; Konopelski and Ufnal 2018). The larger magnitude of change observed at the transcript level (Bcl-2/Bax mRNA) relative to the protein level likely reflects post-transcriptional and post-translational regulation, together with the differing dynamic ranges of quantitative polymerase chain reaction and densitometric protein quantification.

The marked suppression of TNF-α observed with IPA treatment (from 2.25- to 0.70-fold of control at the mRNA level) suggests anti-inflammatory effects beyond simple antioxidant activity. Neuroinflammation is increasingly recognized as a key contributor to both local anesthetic neurotoxicity and hypoxic-ischemic injury, and TNF-α plays a central role in propagating inflammatory cascades and promoting neuronal apoptosis (Block and Hong 2005; Liao et al. 2022). IPA's ability to suppress this pathway may contribute substantially to its neuroprotective efficacy.

These observations also place a microbial metabolite within the pathophysiology of an acute toxic-metabolic brain insult. Because circulating IPA originates from bacterial tryptophan catabolism and varies with diet and microbiota composition (Wikoff et al. 2009; Dodd et al. 2017; Roager and Licht 2018), endogenous IPA status may represent a modifiable metabolic determinant of neuronal vulnerability. Whether baseline IPA concentrations influence susceptibility to drug-induced encephalopathy, and whether exogenous supplementation can be timed to clinical use, are questions raised rather than answered by the present work.

Limitations

Several limitations should be acknowledged. First, because BPV was infused continuously until cardiac arrest, the resulting neuronal injury reflects both direct local anesthetic neurotoxicity and global hypoxic-ischemic damage secondary to circulatory arrest; the present design cannot disentangle these contributions, and the findings should be interpreted as neuroprotection in a combined-injury model rather than against direct neurotoxicity alone. Second, anesthesia was maintained with sevoflurane, which independently modulates both central nervous system and cardiovascular responses and may have influenced the observed outcomes. Third, this lethal continuous-infusion model differs from clinical LAST, in which local anesthetic delivery is discontinued at the onset of toxicity; the results therefore should not be extrapolated directly to clinical LAST management. Fourth, only female rats were studied, so sex-based differences in toxicity and neuroprotection could not be assessed. Fifth, circulating and brain IPA concentrations were not measured, so the exposure achieved by the administered dose remains unverified. Sixth, long-term neurological outcomes were not evaluated, the intraperitoneal route would require adaptation for clinical use, and the modest sample size (n=6 for each group) limits statistical power, particularly for detecting differences among the treatment groups; the optimal timing and dosing of IPA relative to toxicity onset also require further study.

Conclusions

In this experimental rat model, IPA attenuated BPV-induced neuronal injury through anti-apoptotic and anti-inflammatory mechanisms. Given the combined-injury nature of the lethal model and its distance from clinical LAST, these experimental findings should be regarded as hypothesis-generating. Considerable further investigation, addressing model design, dosing, administration route, and timing, is required before any clinical inference can be drawn.

References

Bendheim PE, Poeggeler B, Neria E, Ziv V, Pappolla MA, Chain DG (2002) Development of indole-3-propionic acid (OXIGON) for Alzheimer's disease. J Mol Neurosci 19:213-217. https://doi.org/10.1007/s12031-002-0036-0

Bern S, Weinberg G (2011) Local anesthetic toxicity and lipid resuscitation in pregnancy. Curr Opin Anaesthesiol 24:262-267. https://doi.org/10.1097/ACO.0b013e32834654df

Block ML, Hong JS (2005) Microglia and inflammation-mediated neurodegeneration: multiple triggers with a common mechanism. Prog Neurobiol 76:77-98. https://doi.org/10.1016/j.pneurobio.2005.06.004

Chyan YJ, Poeggeler B, Omar RA, Chain DG, Frangione B, Ghiso J, Pappolla MA (1999) Potent neuroprotective properties against the Alzheimer β-amyloid by an endogenous melatonin-related indole structure, indole-3-propionic acid. J Biol Chem 274:21937-21942. https://doi.org/10.1074/jbc.274.31.21937

Dodd D, Spitzer MH, Van Treuren W, Merrill BD, Hryckowian AJ, Higginbottom SK, Le A, Cowan TM, Nolan GP, Fischbach MA, Sonnenburg JL (2017) A gut bacterial pathway metabolizes aromatic amino acids into nine circulating metabolites. Nature 551:648-652. https://doi.org/10.1038/nature24661

El-Boghdadly K, Chin KJ (2016) Local anesthetic systemic toxicity: continuing professional development. Can J Anaesth 63:330-349. https://doi.org/10.1007/s12630-015-0564-z

Fettiplace MR, Weinberg G (2018) The mechanisms underlying lipid resuscitation therapy. Reg Anesth Pain Med 43:138-149. https://doi.org/10.1097/AAP.0000000000000719

Gitman M, Barrington MJ (2018) Local anesthetic systemic toxicity: a review of recent case reports and registries. Reg Anesth Pain Med 43:124-130. https://doi.org/10.1097/AAP.0000000000000721

Hwang IK, Yoo KY, Li H, Park OK, Lee CH, Choi JH, Jeong YG, Lee YL, Kim YM, Kwon YG, Won MH (2009) Indole-3-propionic acid attenuates neuronal damage and oxidative stress in the ischemic hippocampus. J Neurosci Res 87:2126-2137. https://doi.org/10.1002/jnr.22030

Konopelski P, Ufnal M (2018) Indoles - gut bacteria metabolites of tryptophan with pharmacotherapeutic potential. Curr Drug Metab 19:883-890. https://doi.org/10.2174/1389200219666180427164731

Li J, Yuan J (2008) Caspases in apoptosis and beyond. Oncogene 27:6194-6206. https://doi.org/10.1038/onc.2008.297

Liao MF, Lu KT, Hsu JL, Lee CH, Cheng MY, Ro LS (2022) The role of autophagy and apoptosis in neuropathic pain formation. Int J Mol Sci 23:2685. https://doi.org/10.3390/ijms23052685

Liu Z, Dai X, Zhang H, Shi R, Hui Y, Jin X, Zhang W, Wang L, Wang Q, Wang D, Wang J, Tan X, Ren B, Liu X, Zhao T, Wang J, Pan J, Yuan T, Chu C, Lan L, Yin F, Cadenas E, Shi L, Zhao S, Liu X (2020) Gut microbiota mediates intermittent-fasting alleviation of diabetes-induced cognitive impairment. Nat Commun 11:855. https://doi.org/10.1038/s41467-020-14676-4

Livak KJ, Schmittgen TD (2001) Analysis of relative gene expression data using real-time quantitative PCR and the 2-ΔΔCt method. Methods 25:402-408. https://doi.org/10.1006/meth.2001.1262

Neal JM, Barrington MJ, Fettiplace MR, Gitman M, Memtsoudis SG, Mörwald EE, Rubin DS, Weinberg G (2018) The third American Society of Regional Anesthesia and Pain Medicine practice advisory on local anesthetic systemic toxicity: executive summary 2017. Reg Anesth Pain Med 43:113-123. https://doi.org/10.1097/AAP.0000000000000720

Negatu DA, Gengenbacher M, Dartois V, Dick T (2020) Indole propionic acid, an unusual antibiotic produced by the gut microbiota, with anti-inflammatory and antioxidant properties. Front Microbiol 11:575586. https://doi.org/10.3389/fmicb.2020.575586

Ok SH, Hong JM, Lee SH, Sohn JT (2018) Lipid emulsion for treating local anesthetic systemic toxicity. Int J Med Sci 15:713-722. https://doi.org/10.7150/ijms.22643

Ozcan MS, Weinberg G (2014) Intravenous lipid emulsion for the treatment of drug toxicity. J Intensive Care Med 29:59-70. https://doi.org/10.1177/0885066612445978

Perez-Castro R, Patel S, Garavito-Aguilar ZV, Rosenberg A, Recio-Pinto E, Zhang J, Blanck TJ, Xu F (2009) Cytotoxicity of local anesthetics in human neuronal cells. Anesth Analg 108:997-1007. https://doi.org/10.1213/ane.0b013e31819385e1

Roager HM, Licht TR (2018) Microbial tryptophan catabolites in health and disease. Nat Commun 9:3294. https://doi.org/10.1038/s41467-018-05470-4

Rosenblatt MA, Abel M, Fischer GW, Itzkovich CJ, Eisenkraft JB (2006) Successful use of a 20% lipid emulsion to resuscitate a patient after a presumed bupivacaine-related cardiac arrest. Anesthesiology 105:217-218. https://doi.org/10.1097/00000542-200607000-00033

Shi K, Xia Y, Wang Q, Wu Y, Dong X, Chen C, Tang W, Zhang Y, Luo M, Wang X, Papadimos TJ, Xu X (2013) The effect of lipid emulsion on pharmacokinetics and tissue distribution of bupivacaine in rats. Anesth Analg 116:804-809. https://doi.org/10.1213/ANE.0b013e318284123e

Vasques F, Behr AU, Weinberg G, Ori C, Di Gregorio G (2015) A review of local anesthetic systemic toxicity cases since publication of the American Society of Regional Anesthesia recommendations. Reg Anesth Pain Med 40:698-705. https://doi.org/10.1097/AAP.0000000000000320

Verlinde M, Hollmann MW, Stevens MF, Hermanns H, Werdehausen R, Lirk P (2016) Local anesthetic-induced neurotoxicity. Int J Mol Sci 17:339. https://doi.org/10.3390/ijms17030339

Weinberg GL, VadeBoncouer T, Ramaraju GA, Garcia-Amaro MF, Cwik MJ (1998) Pretreatment or resuscitation with a lipid infusion shifts the dose-response to bupivacaine-induced asystole in rats. Anesthesiology 88:1071-1075. https://doi.org/10.1097/00000542-199804000-00028

Werdehausen R, Braun S, Essmann F, Schulze-Osthoff K, Walczak H, Lipfert P, Stevens MF (2007) Lidocaine induces apoptosis via the mitochondrial pathway independently of death receptor signaling. Anesthesiology 107:136-143. https://doi.org/10.1097/01.anes.0000268389.39436.66

Wikoff WR, Anfora AT, Liu J, Schultz PG, Lesley SA, Peters EC, Siuzdak G (2009) Metabolomics analysis reveals large effects of gut microflora on mammalian blood metabolites. Proc Natl Acad Sci U S A 106:3698-3703. https://doi.org/10.1073/pnas.0812874106

Yang S, Abrahams MS, Hurn PD, Grafe MR, Kirsch JR (2011) Local anesthetic Schwann cell toxicity is time and concentration dependent. Reg Anesth Pain Med 36:444-451. https://doi.org/10.1097/AAP.0b013e318228c835

Youle RJ, Strasser A (2008) The BCL-2 protein family: opposing activities that mediate cell death. Nat Rev Mol Cell Biol 9:47-59. https://doi.org/10.1038/nrm2308

Zhang B, Jiang M, Zhao J, Song Y, Du W, Shi J (2022) The mechanism underlying the influence of indole-3-propionic acid: a relevance to metabolic disorders. Front Endocrinol (Lausanne) 13:841703. https://doi.org/10.3389/fendo.2022.841703

Statements and Declarations

Funding This study was supported by the Dokuz Eylul University Scientific Research Projects Coordination Unit (project no. TTU-2025-3797).

Competing interests The authors declare that they have no conflict of interest with any financial organization regarding the material discussed in the manuscript.

Ethics approval All procedures involving animals were approved by the Dokuz Eylul University Animal Experiments Local Ethics Committee, Izmir, Türkiye (protocol no. 01/2025; approval date: 22 January 2025) and were performed in accordance with the WHO International Guiding Principles for Biomedical Research Involving Animals, the Guide for the Care and Use of Laboratory Animals (National Institutes of Health), the national legal requirements in force in Türkiye, the European Directive 2010/63/EU, and the ARRIVE 2.0 reporting guidelines.

Consent to participate Not applicable.

Consent for publication Not applicable.

Availability of data and material The data supporting the findings of this study are available from the corresponding author upon reasonable request.

Code availability Not applicable.

Authors' contributions Volkan Hanci, Hale Aksu and Faruk Furkan Bank conceived and designed the study. Faruk Furkan Bank and Hale Aksu performed the animal experiments and the induction of bupivacaine toxicity. Faruk Furkan Bank curated the data and wrote the first draft of the manuscript. Serap Cilaker Micili and Selin Nur Cetin performed the histopathological analyses. Beste Balbal and Sefa Kizildag performed the molecular analyses (RT-qPCR and Western blot). Hale Aksu and Sefa Kizildag contributed to the methodology and supervised the respective analyses. Volkan Hanci and Serap Cilaker Micili performed the statistical analysis and prepared Figs. 1–5 and Table 1. Volkan Hanci supervised the study and was responsible for project administration. Hale Aksu, Serap Cilaker Micili and Volkan Hanci revised the manuscript critically for important intellectual content. All authors reviewed and approved the final manuscript.

Declaration of generative AI use During the preparation of this work the authors used a generative artificial intelligence-based large language model (Claude, Anthropic) to improve the language and readability of the manuscript, to assist with reference formatting, and to check the internal consistency of the reported results against the underlying source figures. The tool was not used to generate data, to perform statistical analyses, or to produce any of the numerical results reported in this manuscript. The authors reviewed and edited all content and take full responsibility for the content of the published article.

Table

Table 1 Neuronal density values in the prefrontal cortex and hippocampus by experimental group

Group	Prefrontal cortex (%)	Hippocampus CA1 (%)	Hippocampus CA3 (%)
Control	46.01±0.47	54.02±2.04	46.70±0.30
BPV	29.31±0.59[a]	44.02±2.26[a]	38.60±2.52[a]
BPV+LE	39.21±0.95[b]	50.00±4.81	40.50±2.04
BPV+IPA	40.12±0.47[c]	49.81±1.08	42.80±1.49
BPV+LE+IPA	46.63±0.58[d]	50.31±1.21[b]	44.00±4.58

Data are mean±standard error of the mean. Significance levels correspond to those displayed in Figs. 1–3. [a]P<0.05 versus control. Versus BPV: [b]P<0.01; [c]P<0.001; [d]P<0.0001. *BPV* bupivacaine, *LE* lipid emulsion, *IPA* indole-3-propionic acid, *CA1* cornu ammonis 1, *CA3* cornu ammonis 3

Figure legends

Fig. 1 Histopathological findings in the prefrontal cortex (hematoxylin and eosin staining, ×400). **a** Control group showing normal neuronal morphology with intact cytoarchitecture; **b** BPV group demonstrating marked neuronal degeneration with pyknotic nuclei (arrows) and cytoplasmic eosinophilia; **c** BPV+LE group showing partial preservation; **d** BPV+IPA group with substantially preserved neuronal architecture; **e** combined treatment group with neuronal density comparable to control; **f** quantitative analysis of neuronal density (%). *BPV* bupivacaine, *LE* lipid emulsion, *IPA* indole-3-propionic acid

Fig. 2 Histopathological findings in the hippocampal CA1 region (hematoxylin and eosin staining, ×400). **a** Control group with intact pyramidal neuron layer; **b** BPV group showing extensive neuronal loss and disorganization; **c** BPV+LE group; **d** BPV+IPA group; **e** combined treatment group; **f** quantitative analysis of neuronal density (%). *BPV* bupivacaine, *LE* lipid emulsion, *IPA* indole-3-propionic acid

Fig. 3 Histopathological findings in the hippocampal CA3 region (hematoxylin and eosin staining, ×400). **a** Control group with intact pyramidal neuron layer; **b** BPV group showing extensive neuronal loss and disorganization; **c** BPV+LE group; **d** BPV+IPA group; **e** combined treatment group; **f** quantitative analysis of neuronal density (%). *BPV* bupivacaine, *LE* lipid emulsion, *IPA* indole-3-propionic acid

Fig. 4 Gene expression analysis by real-time quantitative polymerase chain reaction. Relative messenger ribonucleic acid expression levels of **a** B-cell lymphoma 2 to B-cell lymphoma 2-associated X protein ratio, **b** caspase-3, **c** cytochrome c, and **d** tumor necrosis factor-α in brain tissue. Data are normalized to glyceraldehyde 3-phosphate dehydrogenase and presented as fold change relative to the Control group. Values represent mean±standard error of the mean. $P<0.0001$ versus BPV group. *BPV* bupivacaine, *LE* lipid emulsion, *IPA* indole-3-propionic acid

Fig. 5 Protein expression analysis by Western blot. **a** Quantitative densitometric analysis of the B-cell lymphoma 2 to B-cell lymphoma 2-associated X protein ratio; **b** representative Western blot images for B-cell lymphoma 2, B-cell lymphoma 2-associated X protein, and β-actin loading control; **c** quantitative analysis of tumor necrosis factor-α protein levels; **d** representative Western blot images for tumor necrosis factor-α and β-actin. Values represent mean±standard error of the mean. $P<0.01$; $P<0.001$; $P<0.0001$. *BPV* bupivacaine, *LE* lipid emulsion, *IPA* indole-3-propionic acid

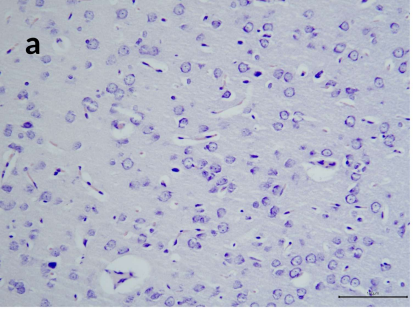
a

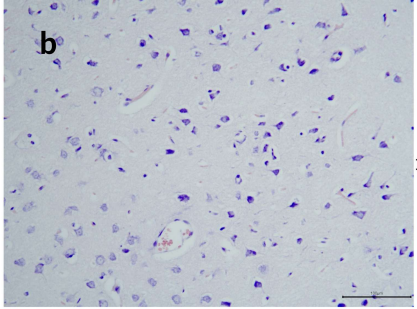
b

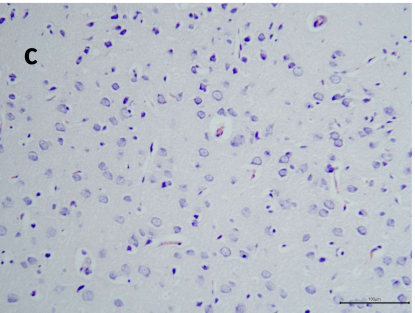
c

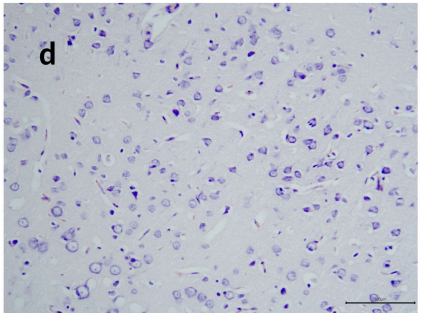
d

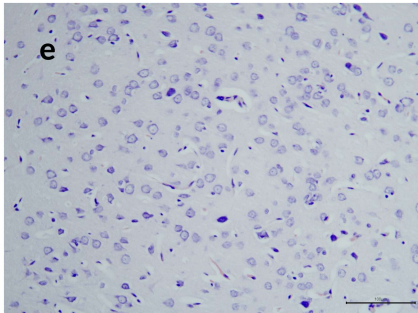
e

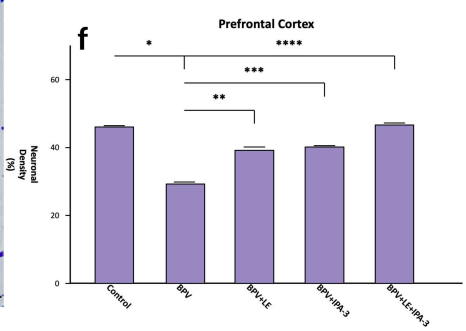
f
Prefrontal Cortex
Neuronal Density (%)
0
20
40
60
*
****
***
**
Control
BPV
BPV+LE
BPV+IPA-3
BPV+LE+IPA-3

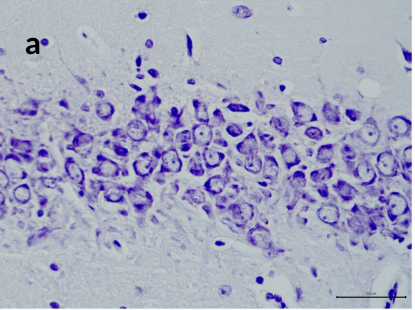
a

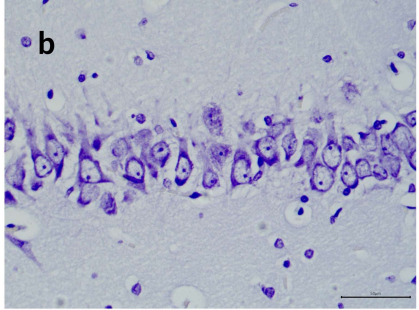
b

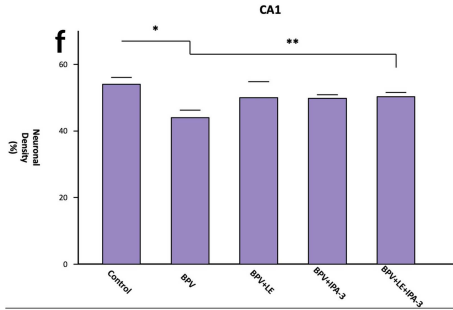
CA1
f
*
**
Neuronal Density (%)
60
40
20
0
Control
BPV
BPV+LE
BPV+IPA-3
BPV+LE+IPA-3

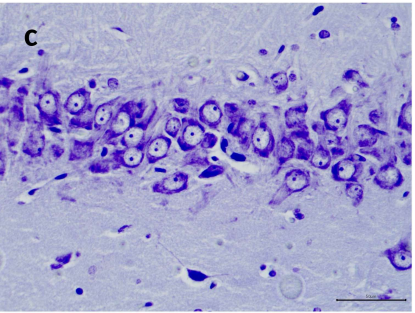
c

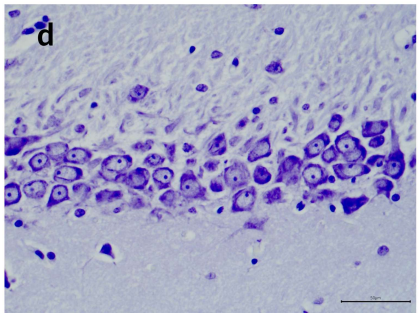
d

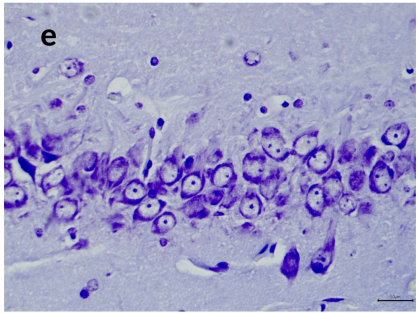
e

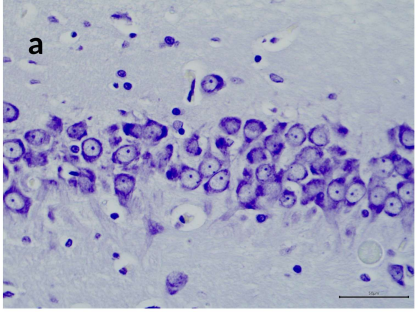
a

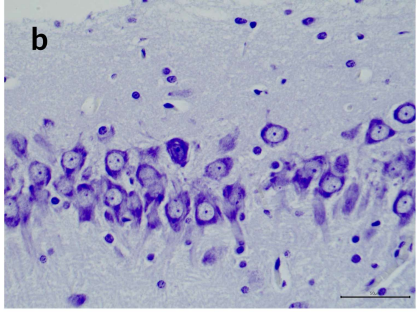
b

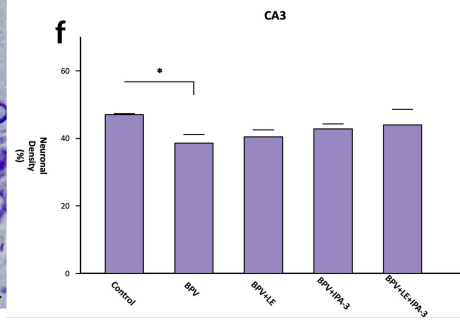
f
CA3
Neuronal Density (%)
60
40
20
0
*
Control
BPV
BPV+LE
BPV+IPA-3
BPV+LE+IPA-3

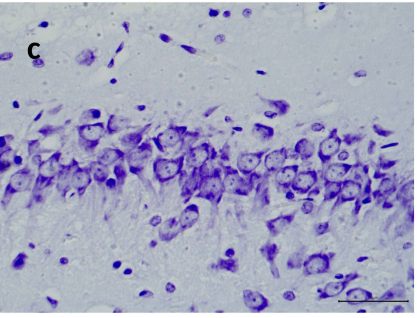
c

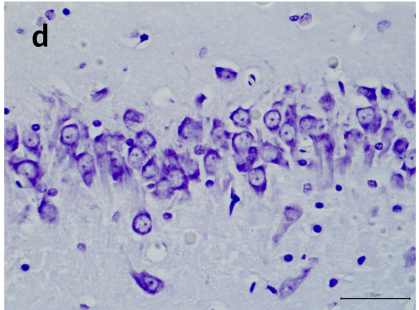
d

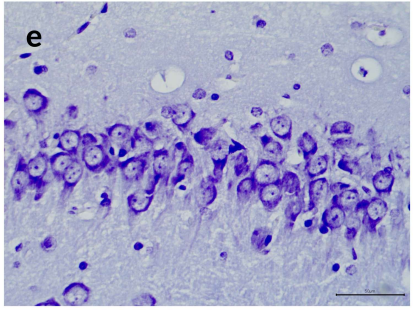
e

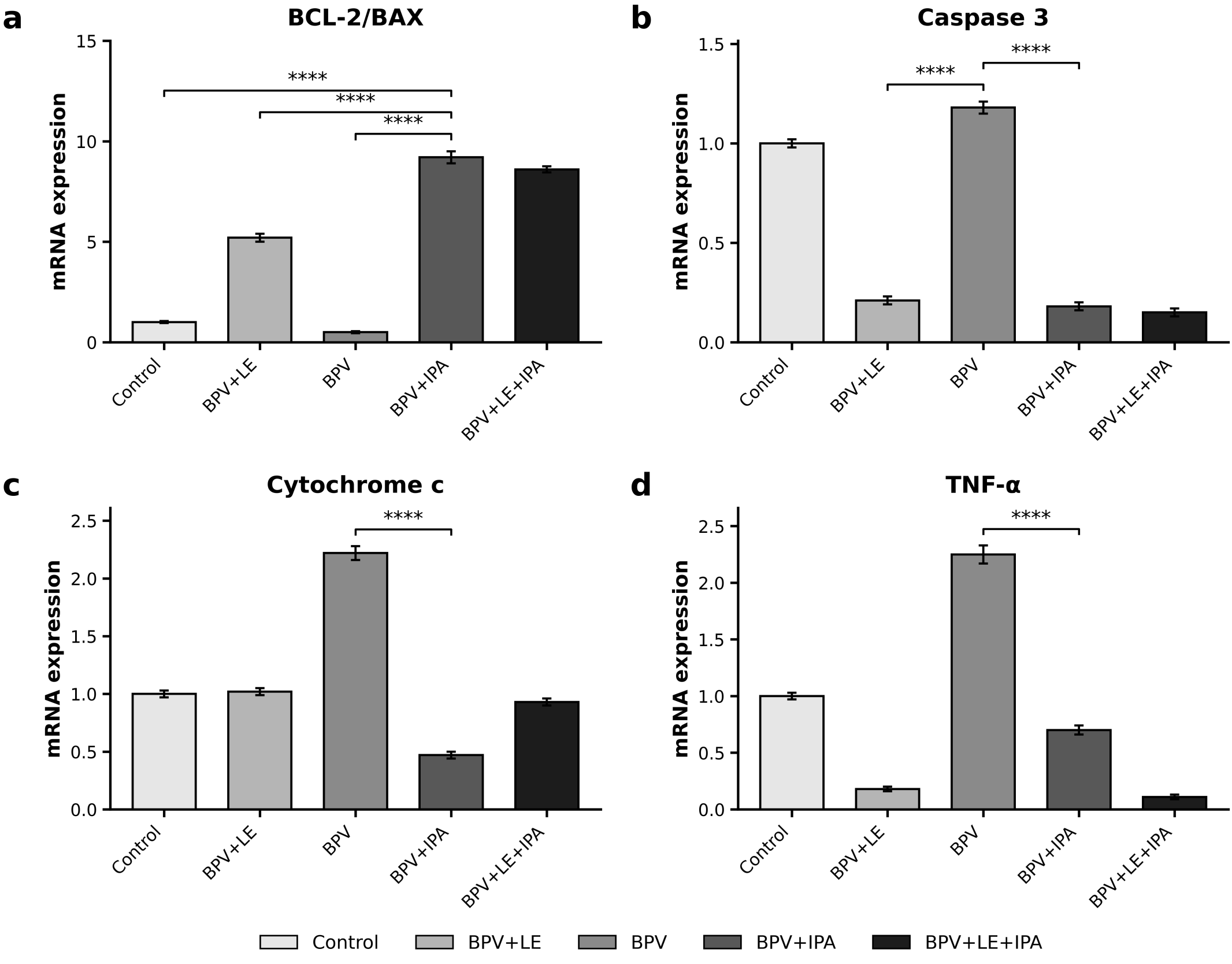
a
BCL-2/BAX
mRNA expression
15
10
5
0
****
****
****
Control
BPV+LE
BPV
BPV+IPA
BPV+LE+IPA
b
Caspase 3
mRNA expression
1.5
1.0
0.5
0.0
****
****
Control
BPV+LE
BPV
BPV+IPA
BPV+LE+IPA
c
Cytochrome c
mRNA expression
2.5
2.0
1.5
1.0
0.5
0.0
****
Control
BPV+LE
BPV
BPV+IPA
BPV+LE+IPA
d
TNF-α
mRNA expression
2.5
2.0
1.5
1.0
0.5
0.0
****
Control
BPV+LE
BPV
BPV+IPA
BPV+LE+IPA
Control
BPV+LE
BPV
BPV+IPA
BPV+LE+IPA

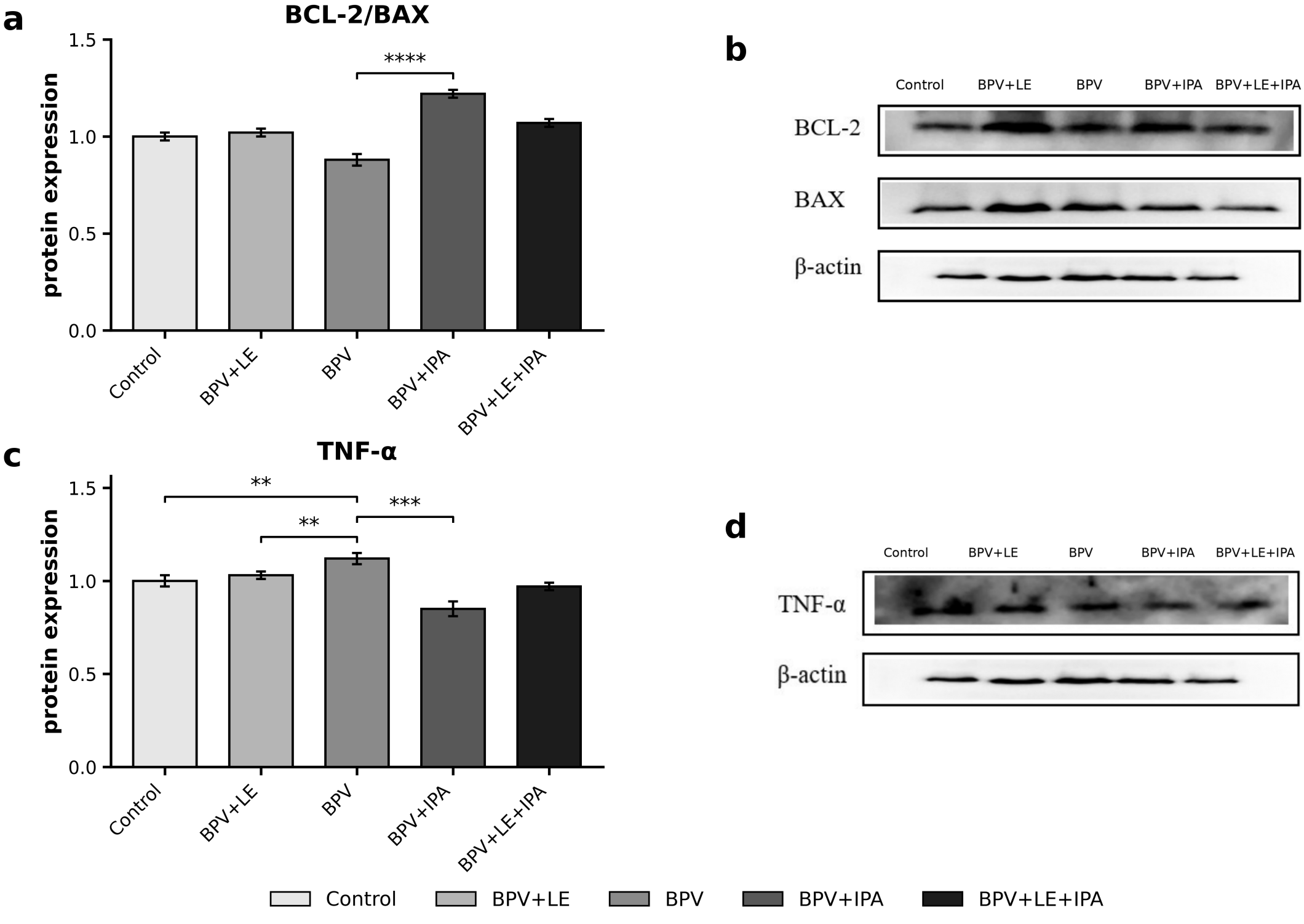
a
BCL-2/BAX
protein expression
1.5
1.0
0.5
0.0
****
Control
BPV+LE
BPV
BPV+IPA
BPV+LE+IPA
b
Control
BPV+LE
BPV
BPV+IPA
BPV+LE+IPA
BCL-2
BAX
β-actin
c
TNF-α
protein expression
1.5
1.0
0.5
0.0
**
**
***
Control
BPV+LE
BPV
BPV+IPA
BPV+LE+IPA
d
Control
BPV+LE
BPV
BPV+IPA
BPV+LE+IPA
TNF-α
β-actin
Control
BPV+LE
BPV
BPV+IPA
BPV+LE+IPA